

Wireless power transfer in the presence of metallic plates: Experimental results

Xiaofang Yu, Torbjørn Skauli, Bjørn Skauli, Sunil Sandhu, Peter B. Catrysse, and Shanhui Fan

Citation: *AIP Advances* **3**, 062102 (2013); doi: 10.1063/1.4809665

View online: <http://dx.doi.org/10.1063/1.4809665>

View Table of Contents: <http://scitation.aip.org/content/aip/journal/adva/3/6?ver=pdfcov>

Published by the [AIP Publishing](#)

A promotional banner for AIP Advances. It features the AIP Advances logo at the top center. To the left, a green diagonal banner reads 'NOW ACCEPTING PAPERS'. Below the logo, the text 'Optical devices for micro- and nano-optics: Fundamentals and applications' is displayed in a large, black, sans-serif font. At the bottom, it says 'Guest Editor: Takasumi Tanabe, Keio University, Japan'. The background is white with a faint, repeating pattern of molecular structures.

NOW ACCEPTING PAPERS

AIP | Advances

Optical devices for micro- and nano-optics:
Fundamentals and applications

Guest Editor: Takasumi Tanabe, *Keio University, Japan*

Wireless power transfer in the presence of metallic plates: Experimental results

Xiaofang Yu,^{1,a} Torbjørn Skauli,^{1,2} Bjørn Skauli,³ Sunil Sandhu,¹
Peter B. Catrysse,¹ and Shanhui Fan^{1,b}

¹*E.L. Ginzton Laboratory, Stanford University, CA 94305, USA*

²*Norwegian Defence Research Establishment, PO Box 25, 2027 Kjeller, Norway*

³*German International School of Silicon Valley, Mountain View, CA 94043, USA*

(Received 6 November 2012; accepted 23 May 2013; published online 3 June 2013)

We demonstrate efficient wireless power transfer between two high Q resonators, especially in a complex electromagnetic environment. In the close proximity of metallic plates, the transfer efficiency stays roughly the same as the free space efficiency with proper designs. The experimental data fits well with a coupled theory model. Resonance frequency matching, alignment of the magnetic field, and impedance matching are shown to be the most important factors for efficient wireless power transfer. © 2013 Author(s). All article content, except where otherwise noted, is licensed under a Creative Commons Attribution 3.0 Unported License. [<http://dx.doi.org/10.1063/1.4809665>]

I. INTRODUCTION

While attempts to transfer electric power wirelessly dates back about 100 years,¹ rapid development of electronic devices has excited renewed interest on this subject.²⁻¹³ In recent years, it has been shown that efficient mid-range wireless transfer can be achieved by utilizing near field magnetic coupling between two identical resonators.^{2-5,7,9-13} Resonance frequency matching, resonance with high quality factors, and fast coupling rate are the keys to achieve high efficiency wireless power transfer.^{2-4,7}

Most of the previous analysis³ and experiments^{4,7} involved transferring power between a source and a receiver both in free space. In certain applications, there is also an interest in transferring energy into a receiver that is placed in a more complex electromagnetic environment.^{2,8} For example, there is a significant interest in the wireless charging of electric vehicles, where a metallic object such as the car body is in the close proximity of the wireless power transfer system.

In a recent paper,² we have shown numerically that efficient wireless power transfer can be achieved in the presence of metallic plates. Here, we confirm this finding experimentally by demonstrating an efficient wireless power transfer system in the presence of metal plates. We show that in order to efficiently transfer power to a receiving resonator located in the vicinity of a metal plate, one could use a symmetric configuration by placing a metal plate in the vicinity of the source resonator, in consistency with the numerical prediction in Ref. 2. Alternatively, high efficiency power transfer can also be accomplished for a system lacking spatial symmetry, by adjusting the resonance frequency and the input impedance of the source resonator. In both cases, the demonstrated maximum efficiency exceeds 94%, over a distance of 60cm, for a resonator with a coil radius of 30cm, operating at 8.4MHz. The key for high efficiency transfer in both cases is to achieve a symmetry in the electromagnetic parameters of the source and receiver resonators.

The paper is organized as follows: Section II presents the coupled mode theory model for the wireless power transfer system. Section III describes the experimental technique and component

^aElectronic mail: xfyu@stanford.edu

^bElectronic mail: shanhui@stanford.edu



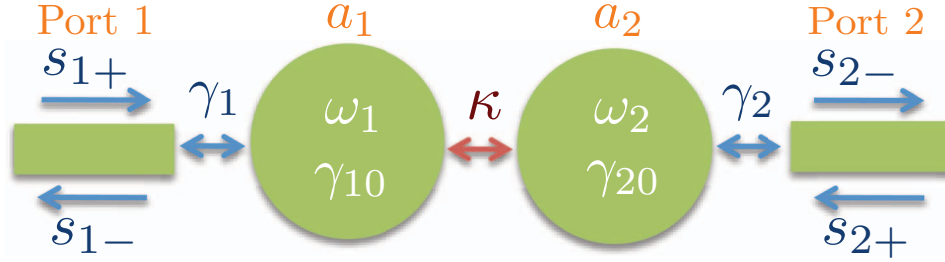


FIG. 1. Coupled mode theory model for the wireless power transfer scheme that utilizes two high-Q resonators. The red arrow represents the wireless power transfer pathway.

characterization. Section IV reports our experimental result of the power transfer in the presence of metallic plates. A brief conclusion is offered in Section V.

II. THEORY

To guide the experimental design and to account for the results, we begin by describing the coupled mode theory model^{2-5,8,14} of the wireless power transfer system. This enables us to highlight the important considerations for achieving efficient power transfer. The model, schematically shown in Fig. 1, consists of two resonances with an input port 1 and an output port 2. The dynamic equations for the system are:

$$\dot{a}_1(t) = (i\omega_1 - \gamma_{10} - \gamma_1)a_1(t) + i\kappa a_2(t) + \sqrt{2\gamma_1}s_{1+}(t) \quad (1)$$

$$\dot{a}_2(t) = (i\omega_2 - \gamma_{20} - \gamma_2)a_2(t) + i\kappa a_1(t) \quad (2)$$

$$s_{1-}(t) = -s_{1+}(t) + \sqrt{2\gamma_1}a_1(t) \quad (3)$$

$$s_{2-}(t) = \sqrt{2\gamma_2}a_2(t) \quad (4)$$

where $|a_1|^2$ corresponds to the energy stored in the source resonance and $|a_2|^2$ corresponds to the energy stored in the receiver resonance. κ is the coupling rate between the source and receiver resonances. $\omega_{1,2}$ are the self-resonant frequencies of the resonators. $\gamma_{1,2}$ are the coupling rates between the resonator and the input/output port. $\gamma_{10,20}$ are the intrinsic decay rates due to absorption/radiation. s_{1+} and s_{2-} are the input and output wave amplitudes, respectively. s_{1-} is the reflective wave amplitude and $s_{2+} = 0$ since no power enters the system from the output port. For a continuous wave input at frequency ω , the power transfer efficiency at steady state becomes:

$$\begin{aligned} \eta &= \left| \frac{s_{2-}}{s_{1+}} \right|^2 \\ &= \left| \frac{\kappa \sqrt{2\gamma_1} \sqrt{2\gamma_2}}{[i(\omega - \omega_1) + (\gamma_1 + \gamma_{10})][i(\omega - \omega_2) + (\gamma_2 + \gamma_{20})] + \kappa^2} \right|^2 \end{aligned} \quad (5)$$

Eq. (5) shows that the resonant transfer scheme requires resonance frequency matching, resonant modes of high quality factor, and a fast coupling rate, in consistency with Refs. 2-4. The optimal operation regime is the “strong coupling” regime when $\kappa/\sqrt{\gamma_{10}\gamma_{20}} > 1$. Moreover, to maximize the transfer efficiency, an optimal configuration consists of the two resonators having the same electromagnetic characteristics, i.e. $\omega_1 = \omega_2 = \omega_0$, $\gamma_1 = \gamma_2 = \gamma$, $\gamma_{10} = \gamma_{20} = \gamma_0$. For such an electromagnetically symmetric configuration, the transfer efficiency is maximized when the operating frequency is ω_0 and $\gamma = \sqrt{\kappa^2 + \gamma_0^2}$:

$$\eta_{max} = \left| \frac{\kappa}{\gamma_0 + \gamma} \right|^2 \quad (6)$$

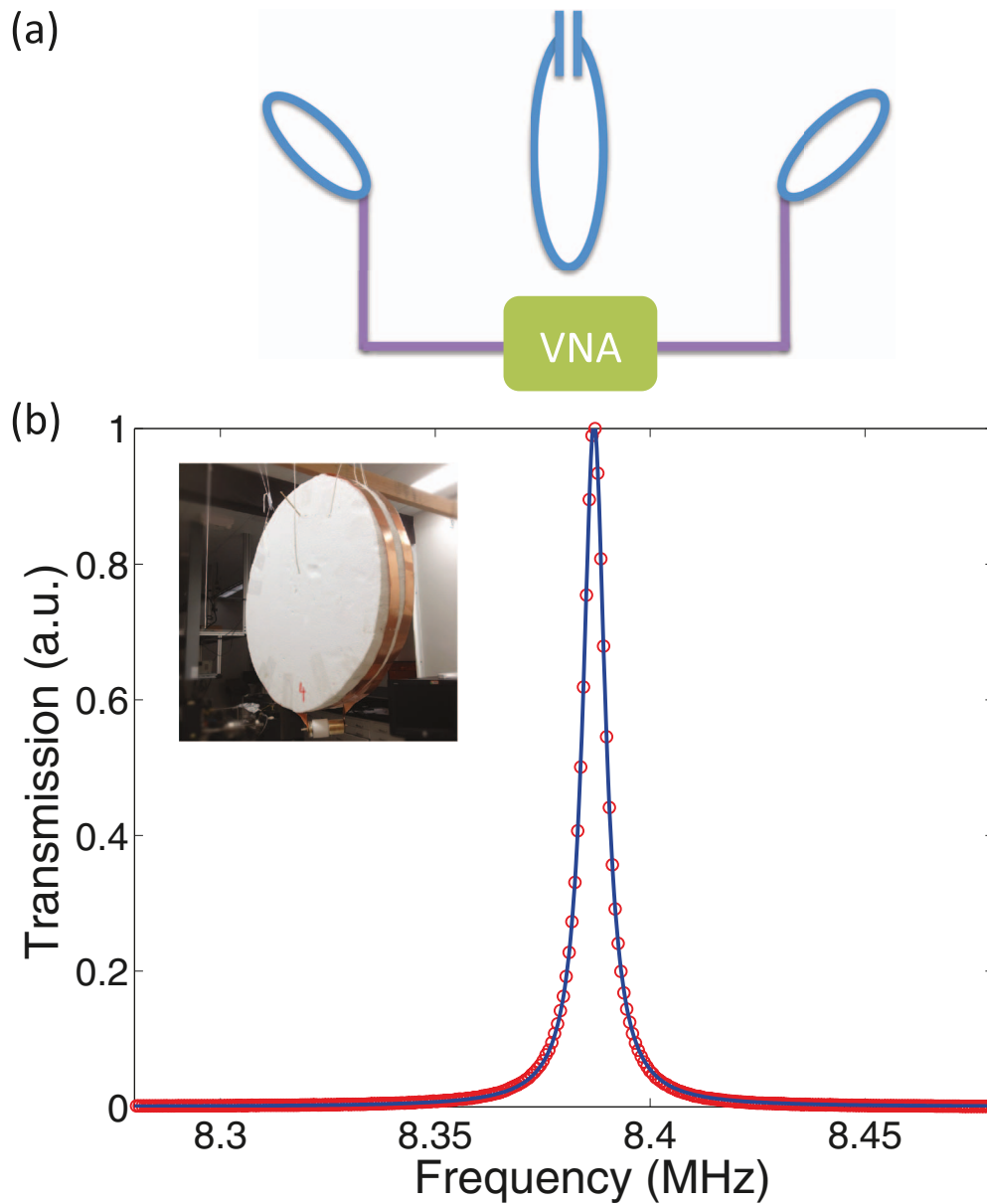


FIG. 2. (a) Schematics of Q measurement setup. (b) The transmission spectrum (red dots are the experiment data and blue line is the Lorentzian fit). The inset is the photo of the resonator we characterize.

In our experiments, we aim to achieve such an electromagnetically symmetric configuration, by either enforcing a geometric symmetry in the system, or by controlling the resonators such that their electromagnetic properties are symmetric, even when the structure itself lacks geometric symmetry.

III. EXPERIMENTAL TECHNIQUE AND COMPONENT CHARACTERIZATION

A. Resonators and their quality factors

One of the essential factors in an efficient wireless power transfer system is the quality factor of the resonators. The quality factor (Q) is related to the intrinsic loss rate (γ_0) of the resonator by $Q = \omega/2\gamma_0$. We measure this intrinsic quality factor using the experimental setup shown in Fig. 2(a). We connect two probing coils to a vector network analyzer (VNA) and orient the coils

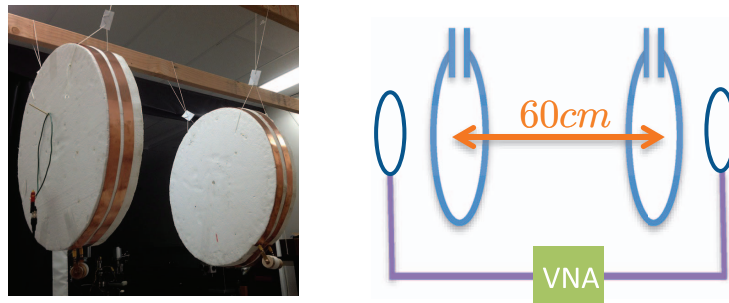


FIG. 3. Photos and schematics of the wireless power transfer experiment. The system consists of two high Q resonators and two coupling coils. The coupling coils are placed right next to the source and receiver resonator serving as the input and output port. Both coupling coils are connected to a vector network analyzer.

to minimize the direct coupling between them. We then place them near the resonator and measure the transmission spectrum between these two probing coils. The quality factor is extracted from the line-shape of the transmission spectrum. This quality factor is for the resonator loaded with the probing coils. By increasing the distance between the probing coils and the resonator, we can reduce the coupling between the probing coils and the resonator. When we reach a point where further reducing the coupling doesn't change the line-shape of the transmission spectrum, we get the intrinsic Q of the resonator.

Fig. 2 is an example of the Q measurement. The resonator shown in the inset of (b) consists of a 2 turn copper ribbon coil with a diameter of about 60cm and a 5 – 70pF adjustable high voltage capacitor. The copper ribbon is 3cm wide and 0.14mm thick. In (b) we show the transmission spectrum. The red dots are the transmission measurement and the blue line is the Lorentzian fit, from which we obtain a resonance frequency of 8.38MHz and a quality factor of 1338. This is in the regime discussed above where the probing coils are sufficiently far away from the resonator. Hence the Q-factor here is the intrinsic quality factor of the resonance.

B. Transfer efficiency measurement and optimization

We measure the wireless power transfer efficiency with the experiment setup shown in Fig. 3. To illustrate the experimental setup and to establish a reference for comparison, we first use this setup to measure the power transfer between two of the resonators characterized in Sec. A without the metallic plates. The separation between the resonators is the transfer distance. Two single-turn wire loops serving as the input and output ports are attached to the VNA and placed next to the source and receiver resonator. The transmission spectrum is directly read out from the VNA.

From the coupled mode analysis, to achieve a high transfer efficiency in such a wireless power transfer system, one needs to do the following : 1) tune the resonators to resonate together ($\omega_1 = \omega_2$); 2) operate at the optimal frequency; 3) maximize the intrinsic quality factor of the resonators (minimize γ_0); 4) orient the resonators along the same axis to maximize the coupling (κ); 5) tune the coupling between the coupling coil and the resonator on each side by adjusting the coupling loop size with the optimal efficiency reached when $\gamma_{1,2} = \kappa - \gamma_0$.

In our experiment, the intrinsic decay rates $\gamma_{10,20}$ of the resonator are fixed by construction, and the coupling coefficient κ is determined once we choose the transfer distance and align the resonators for maximum coupling. To optimize the transfer efficiency, we only need to adjust the size of the coupling coil to affect the input and output coupling rates ($\gamma_{1,2}$), and search for the optimal operating frequency in the transmission spectrum.

Fig. 4 illustrates how we optimize the transfer efficiency by adjusting the size of the coupling loops. The figure shows how the transfer spectra vary as we gradually increase the size of the coupling loops for a transfer distance of 60cm. The red dots are the experimental data and the blue lines are the data fitting based on Eqn. (5). In the case where $\gamma_0 + \gamma \ll \kappa$, we can clearly see the frequency splitting in the transfer efficiency spectra (Fig. 4(a) and 4(b)), but the maximum transfer efficiency

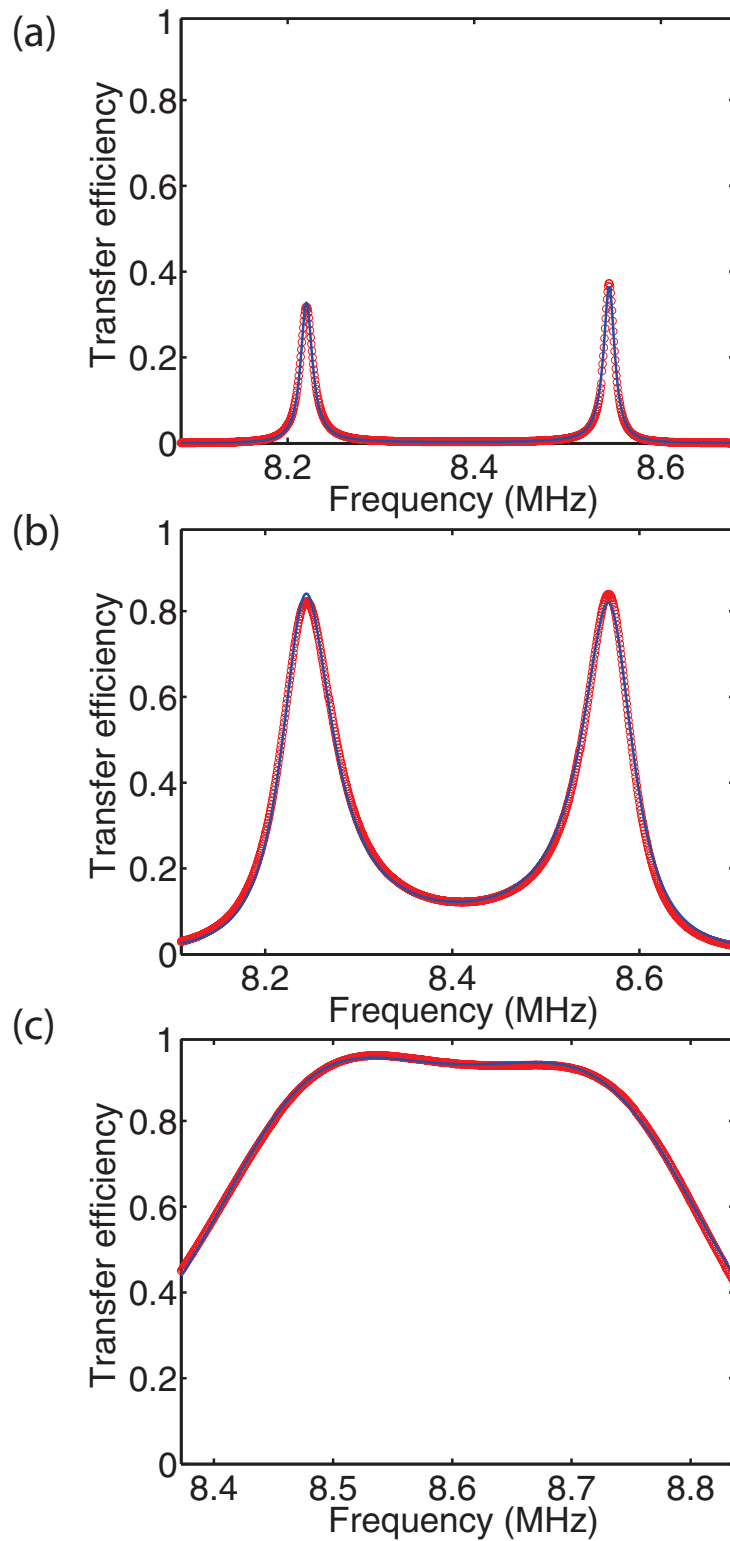


FIG. 4. Transfer efficiency spectra as we increase the coupling loop size when the transfer distance is 60cm. Red dots are experimental data and the blue line is the coupled mode theory model fit. From (a) to (c), we increase the size of the coupling coil.

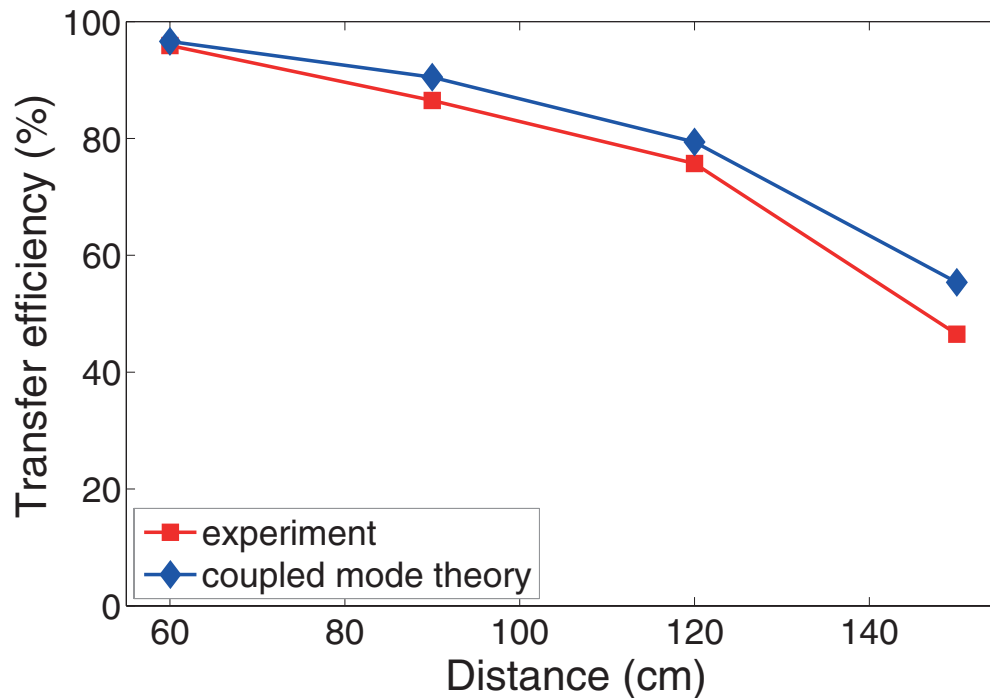


FIG. 5. Maximum transfer efficiency as a function of transfer distance. The red squares are directly measured efficiency. The blue squares are the theoretical result obtained from experimental extracted parameters (κ and γ_0).

is small; when $\gamma_0 + \gamma \approx \kappa$, we no longer see the frequency splitting in the transmission spectrum (Fig. 4(c)), instead we see a wide bandwidth peak. We achieved a maximum transfer efficiency of 96% when the transfer distance is 60cm in our experiment.

The red squares in Fig. 5 shows our experimental measurement of the maximum transfer efficiency versus distance. The blue diamonds are the theoretical predictions of the maximum transfer efficiency at each transfer distance from experimental extracted parameters (κ , γ_0) assuming the optimized conditions ($\kappa = \gamma + \gamma_0$). The result shows that the experimental data is always a few percent lower than the theoretical optimal prediction, which we think is largely due to the noncontinuous tuning of the coupling loops (optimal operation point isn't reached).

IV. POWER TRANSFER IN THE PRESENCE OF METALLIC PLATES: EXPERIMENT

In the previous section, we demonstrated the wireless power transfer in free space. In practice, there are many applications that require the system to work in a rather complex environment, such as in a close proximity of a metallic object, in sea water, etc. In this section, as an important example of a complex environment, we study the influence of a metallic plate on the resonators performance and hence the performance of a wireless power transfer system.

A. Resonance properties as influenced by external environment.

The resonator (Coil 1 in Fig. 6) we characterized in the previous section, differs from some of the resonator geometries that were previously used in wireless power transfer experiments. The experiments in Refs. 4 and 7 used a self-resonant coil with distributed self-capacitance. Here we have also characterized such a self-resonant coil which consists of a 6-turn copper wire that is left open on both ends (Coil 2 in Fig. 6). The coil diameter is 60cm and the wire diameter is 3mm.

We now compare these two resonators. In Fig. 6 we list the resonance frequency and quality factor measurement results under different conditions: free space clear of external objects, with a

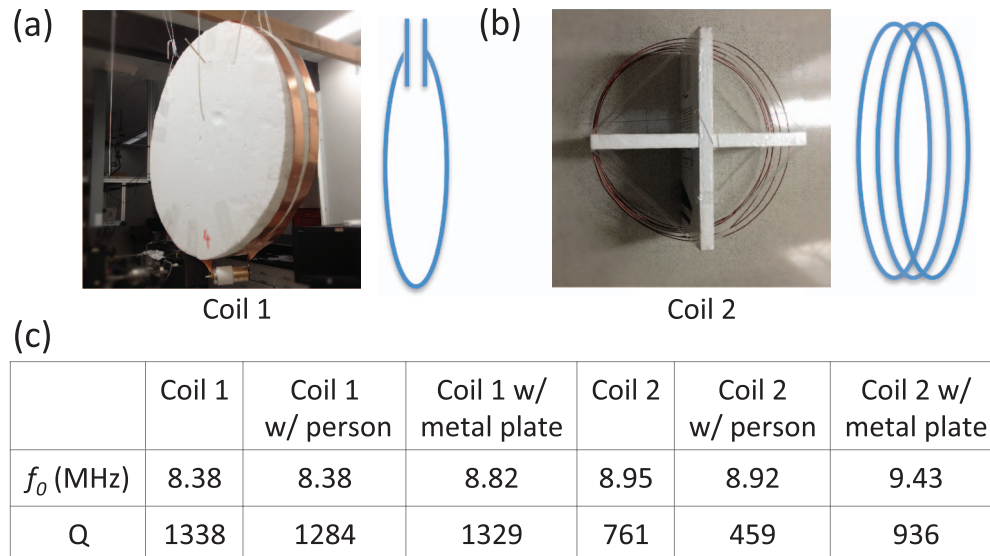


FIG. 6. Photos and schematics of coils with (a) and without (b) an attached capacitor. (c) Resonance frequencies and quality factors of coils in different environment.

large lossy dielectric nearby (e.g. a person standing by), and with a metal plate in a close proximity. When an aluminum plate is placed (parallel to the coil plane) 20cm away from the resonator, the resonance frequency of Coil 1 increases from 8.38MHz to 8.82MHz and the resonance frequency of Coil 2 increases from 8.92MHz to 9.43MHz; the quality factor doesn't change much for Coil 1 but increases by 175 for Coil 2.

When a lossy dielectric comes close to the resonator (such as a person), the resonant frequencies shift as well and the quality factors decrease. From the table in Fig. 6, for Coil 1, neither the resonance frequency nor the quality factor changes much when a person is standing right next to the resonator. However, for Coil 2, its resonance frequency shifts and the quality factor goes down drastically. It turns out that Coil 1 performs better in terms of the robustness due to the better confinement of electric field. Thus, in our experiments, we use Coil 1 in the following power transfer experiment.

A more detailed study on the influence of the aluminum plate on the resonator is shown in Fig. 7. The resonance frequency doesn't change much for Coil 1 unless a metallic object is close (<40cm) to the resonator. The quality factor stays above 1300 for all measured distances from 20cm to 100cm.

B. Wireless power transfer under the influence of environment changes

As we have shown in the previous section, both the resonance frequency and the quality factor of the resonator are influenced by the environment. From coupled mode theory, we can see that the performance of the wireless power transfer system will change as well. In particular, the close proximity of a metallic plate will greatly influence the power transfer system.

In the previous section, we showed that the maximum transfer efficiency of an optimized wireless transfer system (Fig. 3) is 96% over a transfer distance of 60cm. Now we place an aluminum plate at a distance of 20cm from one of the resonators (as shown in Fig. 8(a)) in the optimized system, i.e. close enough to interact with the weak electric fringing fields from the nearest resonator. Since the distances between the plate and the two resonators are different, the self-resonance frequencies of the resonators shift differently and no longer match. According to Eqn. (5), the transfer efficiency will drop as well. Our transfer efficiency measurements do confirm that the transfer efficiency drops (Fig. 8(b)). The maximum transfer efficiency drops from 96% to 37%.

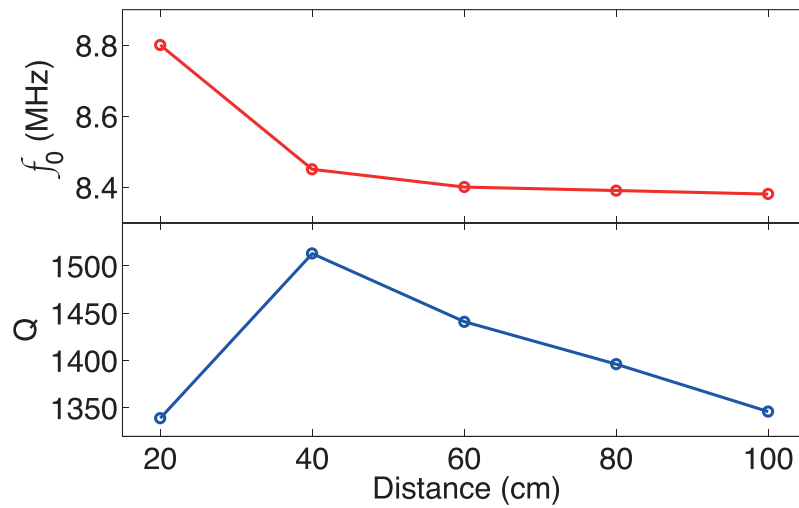


FIG. 7. Resonance frequency and quality factor change with the distance between Coil 1 and the aluminum plate.

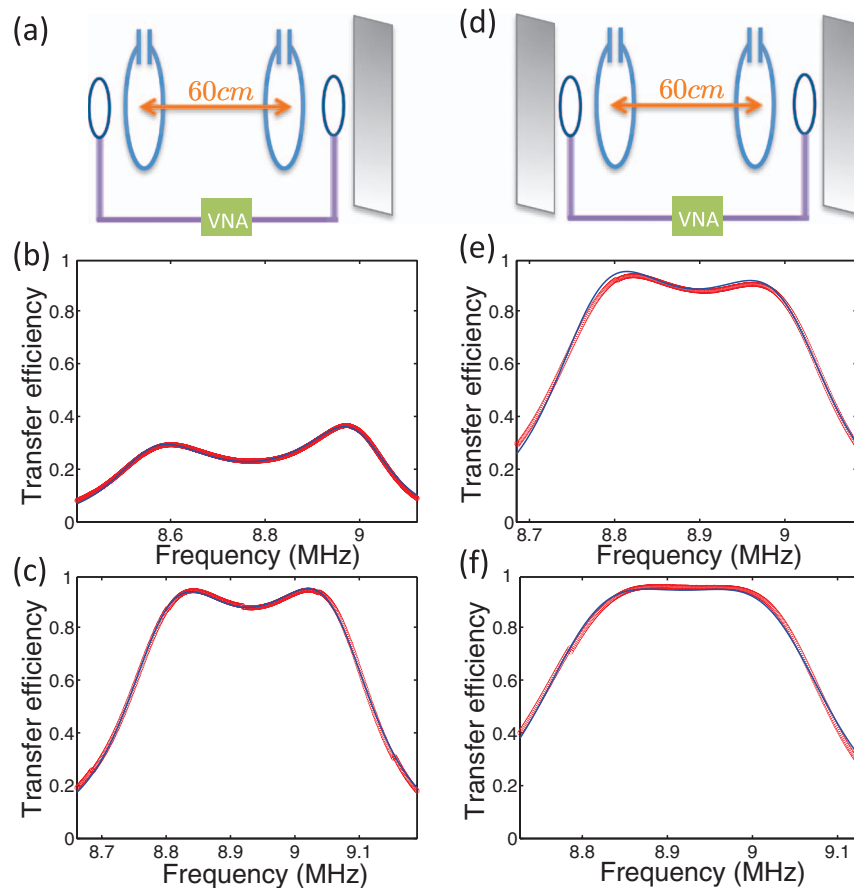


FIG. 8. (a) Schematics of the wireless power transfer system in the close proximity of an aluminum plate. (b) Transfer efficiency spectrum of the wireless transfer system with a metal plate on one side. (c) Transfer efficiency spectrum of the wireless transfer system with an aluminum plate on one side after optimization. (d) Schematics of the wireless power transfer system with two aluminum plates. (e) Transfer efficiency spectrum of the wireless transfer system with aluminum plates on both sides. (f) Transfer efficiency spectrum of the wireless transfer system with aluminum plates on both sides after optimization. Red dots are the experimental data and the blue lines are the coupled mode theory model fit.

We demonstrate two approaches to compensate for the effects of this aluminum plate:

1) Re-tune the resonance frequencies such that the two resonators resonate at the same frequency by adjusting the capacitor. In addition, adjust the coupling coils size to have the impedance match and reach the optimal operating point again. The transfer efficiency spectrum after the re-optimization is shown in Fig. 8(c). With this approach, we can get the transfer efficiency back up to 94%.

2) Place another aluminum plate in a symmetrical way, which automatically matches the resonance frequencies of the resonators without further tuning. The maximum transfer efficiency is 93% without making other changes to the system (spectrum shown in Fig. 8(e)). After fine-tuning the coupling coils, we can get the maximum transfer efficiency back up to 95% (spectrum shown in Fig. 8(f)).

In Fig. 8, we again see excellent agreements between the experimental spectra taken in the presence of the metal plate, and the coupled mode theory. Thus, our coupled mode theory formalism in fact can be applied, and does capture the main physics of wireless power transfer, in the presence of the metal plate.

V. CONCLUSION

In conclusion, we have performed a theoretical and experimental study of a resonant wireless power transfer system. To analyze and optimize the system parameters, we used a coupled mode theory model, which proved to be in excellent agreement with the measured data. We demonstrated a transfer efficiency of 96% over a distance of 60cm. A resonator with a better confinement of the electric field is shown to be a better choice for a robust wireless power transfer system. In addition, we showed that by restoring the electromagnetic symmetry of the system we can overcome the system performance degradation when it is placed in a complex electromagnetic environment.

ACKNOWLEDGMENT

This work is supported by the Global Climate and Energy Project (GCEP) at Stanford University and TomKat Center for Sustainable Energy at Stanford. The authors acknowledge Dr. Sven Beiker and Dr. Richard Sassoon for useful discussions.

¹ N. Tesla, U. S. patent 1,119,732 (1914).

² X. Yu, S. Sandhu, S. Beiker, R. Sassoon, and S. Fan, *Appl. Phys. Lett.* **99**, 214102 (2011).

³ A. Karalis, J. Joannopoulos, and M. Soljačić, *Annals of Physics* **323**, 34 (2008).

⁴ A. Kurs, A. Karalis, R. Moffatt, J. D. Joannopoulos, P. Fisher, and M. Soljačić, *Science* **317**, 83 (2007).

⁵ R. E. Hamam, A. Karalis, J. Joannopoulos, and M. Soljačić, *Annals of Physics* **324**, 1783 (2009).

⁶ L. Peng, O. Breinbjerg, and N. Mortensen, *J. of Electromagn. Waves and Appl.* **24**, 1587 (2010).

⁷ A. P. Sample, D. A. Meyer, and J. R. Smith, *IEEE Trans. Industrial Electronics* **58**, 544 (2011).

⁸ S. Kim, J. S. Ho, and A. S. Y. Poon, *Appl. Phys. Lett.* **101** (2012).

⁹ B. Wang, K. H. Teo, T. Nishino, W. Yezunis, J. Barnwell, and J. Zhang, *Appl. Phys. Lett.* **98**, 254101 (2011).

¹⁰ Y. Urzhumov and D. R. Smith, *Phys. Rev. B* **83**, 205114 (2011).

¹¹ E. Thomas, J. Heeb, C. Pfeiffer, and A. Grbic, *IEEE Trans. Circuits and Syst. I* **59**, 2125 (2012).

¹² D. Huang, Y. Urzhumov, D. R. Smith, K. H. Teo, and J. Zhang, *Journal of Applied Physics* **111**, 064902 (2012).

¹³ L. Chen, S. Liu, Y. C. Zhou, and T. J. Cui, *IEEE Trans. Ind. Electron.* **60**, 339 (2013).

¹⁴ H. Haus, *Waves and Fields in Optoelectronics* (Princeton Hall, 1984).